International Journal for Housing Science and Its Applications
Publish August 10, 2025. Volume 46, Issue 4 Pages 8075-8085

https://doi.org/10.70517/ijhsa464691

Dynamic Characteristics and Simulation Modeling of Tennis Serve Trajectories

Zhengjian Gao[1,*] and Dongqi Liu[2]
[1] Yanching Institute of Technology, Sanhe, Hebei, 065201, China
[2] Public Teaching Department, China University of Labor Relations, Beijing, 100048, China
Corresponding authors: (e-mail: gzj323@163.com).

Abstract The kinematic characteristics and patterns of excellent serve motions are currently a hot topic in research on serve quality in tennis. This study selected 10 male national-level tennis athletes as experimental subjects. Based on research needs, the serve technique was defined and divided into four time points and three stages. The origin of the coordinate system, the initial state of the racket, and the definition of racket rotation were determined at the experimental site. By analyzing the force conditions during tennis movement, the forces influencing the tennis trajectory were identified. Based on the force conditions, the movement process was reconstructed, and a motion equation was established for the tennis movement process, thereby proposing a tennis kinematic model. In the simulation experiments and analysis of the proposed model to the topspin serve action of the tennis ball at different landing points of the research sample, it is found that the ball speed has a great influence on the drag coefficient, and when the tennis ball speed is 40m*s-1, the drag coefficient increases to 0.1347 accordingly.

Index Terms tennis biomechanical model, tennis serve trajectory, serve technique, dynamics

I. Introduction

Tennis is often referred to as the second most gentlemanly sport in the world. In recent years, with the increasing number of high-level professional tennis tournaments held in various regions and the intense competition among tennis players on the global stage, the sport has seen broader development worldwide, attracting many non-athletes to participate [1]-[3]. As more people join the sport of tennis, research on tennis has also attracted the participation of more researchers. Globally, tennis research primarily focuses on several areas, including the development of tennis [4], [5], technical analysis of tennis [6], [7], prediction of tennis performance [8], [9], analysis of tennis training movements [10], and tennis-related injuries [11]. With the rapid development of computer technology and the accumulation of tennis practice experience, the use of computer simulation technology to simulate and model tennis trajectories has become a theoretical hotspot in tennis research. The key to winning in tennis lies in the direct scoring ability of the serve and the scoring strength of the return strategy system being superior to the opponent's [12], [13]. Given the significant role of the serve in tennis matches, it has received considerable attention from the global tennis community and has been the subject of extensive in-depth research. In tennis practice, the serve is one of the most technically and biomechanically complex movements in the game, requiring strength, speed, accuracy, timing, and angle of contact, as well as the coordinated action of multiple joints, muscle groups, and the nervous system [14]-[16]. During the serve, the trajectory can be freely controlled through serving technique, and if controlled appropriately, it can lead to scoring and victory [17]. Therefore, conducting a dynamic analysis of the tennis serve trajectory enables athletes to better master the serving technique.

Tennis serves primarily consist of three types: flat serves, side spin serves, and topspin serves. Every point in tennis begins with a serve, making it the only tennis technique unaffected by the opponent. In professional tennis, relying on serves to gain an advantage or even score directly is an important strategy [18], [19]. Reference [20] utilized an inertial measurement unit for biomechanical analysis of tennis serves, employing wearable inertial measurement unit clothing to collect kinematic data, thereby providing serving guidance for tennis athletes. This demonstrates the critical importance of dynamic analysis of serving movements. Literature [21] combines image processing technology and wireless sensor technology to mark the coordinates of the racket handle joint in tennis videos, thereby studying the serve trajectory. An improved support vector machine was used to construct a tennis serve model to simulate tennis serve behavior. Literature [22] uses frame-to-frame difference technology to locate tennis serves, detect specified shoulder markers on the court, and combines an enhanced support vector machine to build a tennis serve model for evaluation and inspection of marker trajectories. Reference [23] studied the two-dimensional motion trajectory characteristics of ball release in different serve types at different positions in the

Djokovic zone and advantage ball zone, based on three sets of data: the ball release point, the vertical peak of the ball's trajectory, and the contact point between the racket and the ball. Literature [24] designed a tennis serve trajectory capture algorithm, primarily using computer 3D vision capture and a mean filter to collect and process tennis serve trajectory images. After wavelet multiscale decomposition, the initial tennis serve trajectory image was completed using magnitude and phase angle values.

This paper first selects 10 male national first-class tennis players as experimental subjects, compiles the basic information of the 10 athletes, and uses this as the research sample. At the same time, it establishes the criteria for dividing the timing and stages of the serve technique, analyzes the origin of the coordinate system and the rules for defining the racket in this study, and designs the data collection process for the experiment. Next, the paper provides a detailed analysis of the three force analysis scenarios for a spinning tennis ball during flight, proposes the state equations for the tennis ball's motion process, and constructs a kinematic model for tennis ball motion. It further describes the changes in various parameters—including force application speed and center of gravity at the point of impact—during the “back swing” phase and the racket swing phase of the side-spin serve for different landing points, and analyzes the displacement and velocity characteristics of the body's motion during this process. Finally, based on the characteristics of the surrounding flow field when the tennis ball is in different states of motion, this paper uses the established model to analyze the relationship between the drag coefficient and the tennis ball's velocity and rotational velocity.

II. Research Subjects and Research Preparation

II. A.Experimental subjects

The subject of this study is the first and second serve techniques of male national first-class tennis players. The experimental sample consisted of 10 male national-level tennis players (age range: 15–23 years, average age: 19.5 ± 3.1 years, training duration: 10.5 ± 2.1 years, weight: 75.5 ± 6.3 kg, height: 184.1 ± 5.5 cm, dominant hand: right). No history of injury or illness in the three months prior to the test. All participants voluntarily participated in this experiment and were informed of the experimental procedures and content. The basic information of the 10 athletes is shown in Table 1.

Table 1: Basic information of athletes

	Height (cm)	Weight(kg)	Age	Training years
Average value	184.1	75.5	19.5	10.5
Standard deviation	4.8	5.9	3.0	2.2
Maximum value	189.7	83.3	23.1	15.2
Minimum value	180.6	62.8	15.3	9.1

II. B.Phase Division

Research on serving techniques begins with the division of movement cycles, with the three-stage division currently being the mainstream approach. Based on the research objectives of this paper, serving techniques are defined as the following four moments and three stages, as shown in Figure 1.

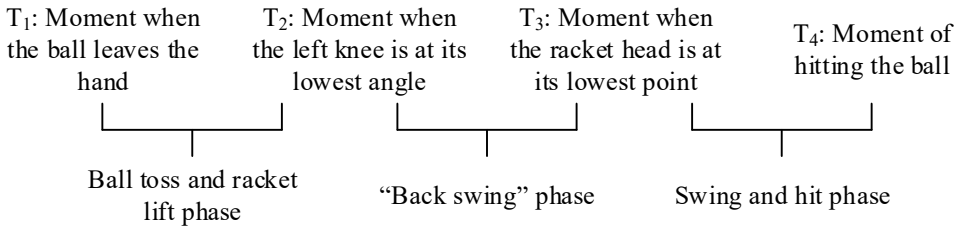

Figure 1: Division of stages for serving technique movements

where T_1: the moment the ball leaves the hand, T_2: the moment when the left knee is at its minimum angle of flexion, T_3: the moment when the racket head is at its lowest point, T_4: the moment of impact.

Ball release and racket raise phase $(T_1 - T_2)$: From the moment the ball leaves the hand to the moment of minimum left knee flexion.

“Scratching the back” phase $(T_2 - T_3)$: From the moment of minimum left knee flexion angle to the moment when the racket head is at its lowest point.

Racket swing and ball strike phase $(T_3 - T_4)$: From the moment when the racket head is at its lowest point to the moment of ball strike.

II. C. Origin of the coordinate system and definition of the racket

The origin of the coordinate system is the midpoint of the baseline. The positive direction of the X-axis is parallel to the right side of the midpoint of the baseline (the negative direction is to the left). The positive direction of the Y-axis is perpendicular to the baseline from the midpoint of the baseline (the negative direction is backward). The positive direction of the Z-axis is perpendicular to the baseline from the midpoint of the baseline (the negative direction is downward). See Figure 2 for the experimental site.

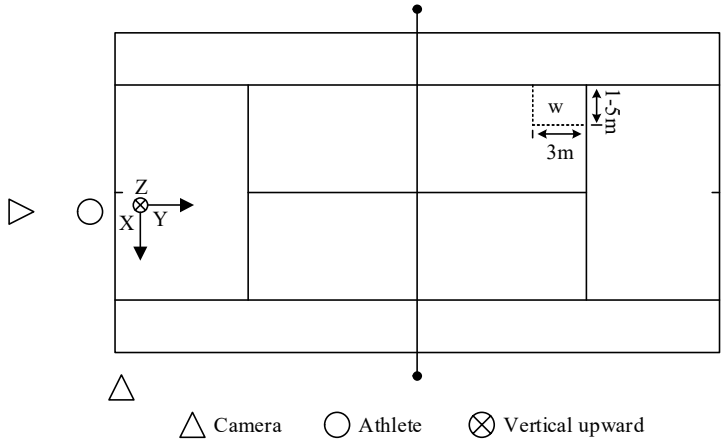

Figure 2: Experimental site

Regarding the racket, Euler angles ($Z-Y-X$ rotation order) are used to describe the rotational state of the racket at the moment of impact. The center point of the racket is obtained by connecting the midpoints of the left and right sides of the racket. The Z axis direction of the racket is defined as pointing upward from the center point toward the racket head, the Y-axis direction is the dot product of the vector from the center point to the right side of the racket and the Z-axis, and the X-axis direction is the dot product of the Z-axis and the Y-axis. The positive or negative values of these data only indicate direction, not magnitude. The original state of the racket is defined in Figure 3 (the rotation arrow points in the positive direction, and the opposite direction is negative).

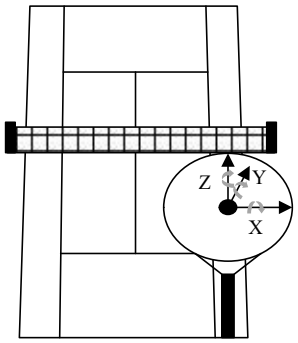

Figure 3: Definition of the original state of the racket

This paper studies the details of the racket rotation definition shown in Figure 4, where the rotation direction is positive, from left to right, respectively, racket downward pressure (X axis), racket right rotation (Y axis), and racket outward rotation (Z axis). The opposite direction is racket upward tilt, racket left rotation, and racket inward rotation.

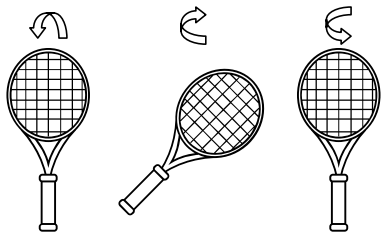

Figure 4: Racket condition

II. D.Experimental Data Collection Process

The target serving areas used in existing studies primarily include three sizes: $1\times1m^2$, $1.5\times1.5m^2$, and $2\times1m^2$. To facilitate the expansion of the testing protocol, the outer corner of Zone 1, including the first and second serves, is defined as a $1.5\times3m^2$ target area for measurement. Prior to the test, athletes undergo a 30-minute warm-up followed by a 10-minute specific serving training phase using their own rackets. Once in a ready state, participants enter the formal testing phase. Athletes are instructed to perform two powerful serves to the designated target area in the specified order of first and second serves. Athletes serve “first serves” and “second serves” rather than being restricted to serving “flat serves,” “side spin serves,” or “topspin serves.” In this way, athletes are instructed to maintain the first and second serves they most frequently use in matches to deliver the ball to the target position. This helps ensure serve effectiveness and minimizes the likelihood of athletes adopting unusual movement patterns due to overly restrictive instructions. Subsequently, one successful serve is selected from the first and second serves jointly determined by the coach and athlete for further analysis.

III. Tennis Kinesiology Model

Among the three types of tennis serves, the side spin serve and the topspin serve are relatively easy to understand, as the ball's own rotation, generated by the racket's impact, is either sideways or upward. The flat serve also has spin, but since the primary force applied by the racket is through the center of the ball, the ball's spin is minimal, hence the term “flat serve.” However, as the ball speed increases, the ball's speed also increases. Due to the differing air resistance encountered by the ball during its flight, the ball will develop some spin.

III. A. Analysis of Forces Acting on a Spinning Ball in Flight

Under ideal conditions, when serving with a flat hit, the tennis ball has no spin. Therefore, when spin is not considered, the tennis ball is primarily affected by two forces during flight: the downward force of gravity F_g and the air resistance F_d acting in the opposite direction of the ball's motion. In practice, the tennis ball does generate some spin during its motion. When considering the spin of the tennis ball during its motion, it is not only affected by gravity F_g and air resistance F_d but also by the Magnus force F_m The direction of the Magnus force varies depending on the direction of spin. During a flat serve, the lateral forces acting on the ball are largely balanced, as the two forces are opposite and cancel each other out. However, the forces acting on the ball vertically are unbalanced. On one hand, this is due to the impact force at the point of contact (during a flat serve, the ball is struck on the upper rear portion). On the other hand, the ball's trajectory is downward, resulting in different vertical forces. This is also the reason for the generation of the Magnus force. Therefore, when analyzing the forces acting on the ball during a flat serve, it is sufficient to consider only the case where the ball generates topspin. In this study, only the case of topspin on the tennis ball is considered for force analysis.

The force conditions on the tennis ball during its motion are shown in Figure 5.

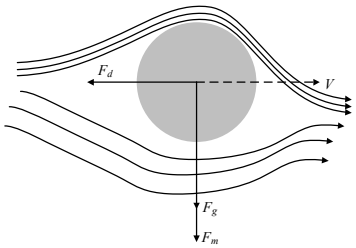

Figure 5: The force conditions during tennis

The following is a detailed analysis of the three stress situations:

(1) Gravity $F_g = mg$, m is the mass of the tennis ball, g is the acceleration of local gravity, $g = 9.8m/s^2$, the tennis ball is always under the action of gravity, and the direction is vertical downward.

(2) Air resistance F_d, air resistance is always opposite to the direction of motion, air resistance is calculated as follows equation (1):

$$F_d = \frac{1}{2} C_d \rho A \|V\| V \tag{1}$$

where C_d is the drag coefficient, ρ is the air density, A is the frontal area of the tennis ball, $A = \frac{\pi d^2}{4}$ (d is the diameter of the tennis ball), and V is the velocity of the tennis ball.

(3) Magnus force F_m.

The reason why a rotating object can generate a lateral force is that the rotation of the object causes the surrounding fluid to rotate, resulting in an increase in fluid velocity on one side of the object and a decrease on the other side. According to Bernoulli's principle, an increase in fluid velocity leads to a decrease in pressure, while a decrease in fluid velocity leads to an increase in pressure. This creates a pressure difference on the lateral side of the rotating object, thereby generating a lateral force. Since the lateral force is perpendicular to the direction of motion, it primarily alters the direction of flight speed, acting as a centripetal force during motion and causing a change in the object's flight direction. The Magnus force is perpendicular to the angular velocity direction and perpendicular to the direction of motion. Therefore, when a tennis ball is hit with topspin, the force acts downward. The formula for the Magnus force is given by Equation (2):

$$F_m = \frac{1}{2} C_l \rho \frac{d}{2} A \|\omega\| \times \|V\| \frac{\omega \times V}{\|\omega \times V\|} \tag{2}$$

Among them, C_L is the lift coefficient, and ω is the angular velocity of the tennis ball's spin.

III. B. Model Establishment

A tennis ball in motion can be approximated as a six-degree-of-freedom spherical rigid body. The tennis ball is primarily subjected to three forces: the Magnus force, gravity, and air resistance. Therefore, the motion of the tennis ball can be described by equations (3)–(6):

$$m\dot{\vec{V}} = \vec{F_d} + \vec{F_m} + \vec{F_g} \tag{3}$$

$$\vec{F_d} = \frac{1}{2} C_d \rho A \|V\| V \tag{4}$$

$$\vec{F_m} = \frac{1}{2} C_L \rho \frac{d}{2} A \|\omega\| \times \|V\| \frac{\omega \times V}{\|\omega \times V\|} \tag{5}$$

$$\vec{F_g} = \begin{bmatrix} 0 & 0 & -mg \end{bmatrix}^T \tag{6}$$

Based on the typical parameters in equations (3)-(6), the typical values of gravity, air resistance, and Magnus force can be calculated. The gravitational force F_g is $0.5586N$, the air resistance F_d is $0.0267N - 0.0567N$, and the Magnus force F_m is $0N - 0.1398N$. It can be seen that for a rotating ball, the Magnus force and air resistance acting on the tennis ball are non-negligible. The motion of the tennis ball can be described by the state equation in equation (7):

$$\begin{bmatrix} \dot{x} \\ \dot{y} \\ \dot{z} \\ \dot{V}_x \\ \dot{V}_y \\ \dot{V}_z \end{bmatrix} = \begin{bmatrix} V_x \\ V_y \\ V_z \\ -k_d \|v\| v_x \\ -k_d \|v\| v_y \\ -k_d \|v\| v_z - k_m \|v\| v_z - k_g g \end{bmatrix} \tag{7}$$

Among them are equations (8)-(9):

$$k_d = \frac{1}{2m} \rho A C_d \tag{8}$$

$$k_m = \frac{d}{4m} \rho A C_L \frac{\|\omega\| \times \|V\|}{\|\omega \times V\|} \tag{9}$$

IV. Analysis and Simulation Experiment of Tennis Serve Trajectory

IV. A. Different stages of the tennis topspin serve motion

IV. A. 1) The "scratching one's back" stage

The changes in joint angles during the "scratching the back" phase are shown in Table 2, where: (V1) arm swing angle, (V2) elbow flexion, (V3) upper arm flexion angle, (V4) upper arm abduction, (V5) horizontal abduction, (V6) trunk rotation, (V7) trunk inclination, and (V8) knee flexion. Significant differences in the magnitude of joint angle changes were observed across different serve landing points, with joint angles increasing in the order of outer angle—chase—inner angle. The joints with the largest changes in angle were (V2) elbow flexion angle (34.5°), (V1) racket arm angle (24.3°), (V6) trunk rotation angle (34.2°), and (V7) trunk tilt angle (26.1°). Larger angles indicate greater force exertion at the corresponding joint, with the order of force magnitude being inner angle serve (T), body serve (Body), and outer angle serve (Wide).

Table 2: Angle Changes of Each Link

	Wide		Body		T	
	Mean	SD	Mean	SD	Mean	SD
V1	24.3*	3.3	24.2**	3.4	31.1***	2.6
V2	34.5*	4.2	35.1**	3.9	39.1***	3.1
V3	16.9*	3.5	19.9**	3.7	22.1***	4.2
V4	13.3*	4.4	16.3**	4.4	17.9***	6.4
V5	9.4*	3.4	9.8**	3.9	12***	4.5
V6	34.2*	4.5	34.8**	2.9	40***	2.1
V7	26.1*	2.7	28.1**	2	30.2***	4.1
V8	28.1*	2.9	29**	3.5	29.8***	5.5

IV. A. 2) Swing and hit the ball stage

See Figure 6 (a) for the force speed of different human joints in the hitting stage, and see Figure 6 (b) for the force speed of different links, wherein the human body links include: (A1) foot, (A2) knee, (A3) hip, (A4) shoulder, (A5) elbow, (A6) wrist, and different links are: (B1) head and (B2) ball speed. When serving at different landing points, the overall force sequence of the players is relatively smooth, which conforms to the whipping mechanics principle of the serving technique, and the speed of each joint part is superimposed in turn and gradually transmitted to the hitting point.

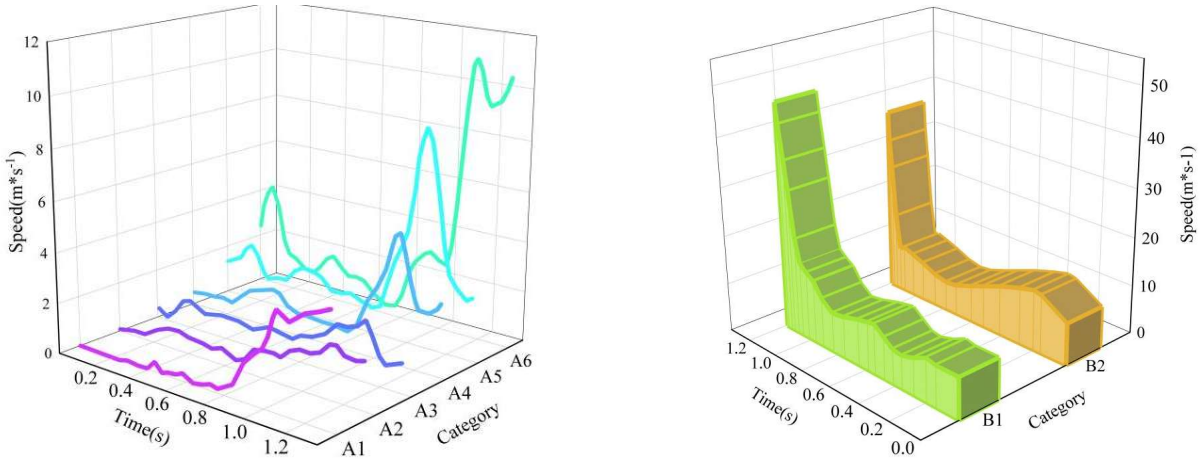

(a) The speeds of different human joints

(b) The speed of different serving segments

Figure 6: Sequence Diagram of Body Joints

The hitting points and center parameters for serves with different landing points are shown in Table 3. The velocity components in each direction from the outer corner to the inner corner are as follows: outer corner (side spin) > body (side spin) > inner corner (side spin), inner corner (top spin) > body (top spin) > outer corner (top spin). Additionally, there are significant differences in hitting angles: inner corner (Angle) < body-facing (Angle) < outer

corner (Angle). Ball speed also shows significant differences across different landing points. Thus, the key indicators determining the landing point of the serve are the angle and velocity components at the moment of impact.

The ratio of the hitting point to height is 1.35 for the outer corner, 1.26 for the body-following, and 1.19 for the inner corner. The height of the hitting point varies significantly among different landing points, with inner corner < body-following < outer corner. Based on the horizontal projection point position, the hitting point position gradually shifts to the right front from the inside to the outside. The distance from the left toe to the hitting point is inner angle < body angle < outer angle.

The average jump height for side-topspin serves is 0.25 ± 0.01 m, and there are significant differences in jump height across different landing points (T: 0.20 ± 0.02 m vs. B: 0.25 ± 0.02 m vs. W: 0.30 ± 0.03 m). From the inner angle to the outer angle, the jump height during serving gradually increases, indicating increased leg power.

Table 3: Parameters of BI and COG at Different Locations

	Wide		Body		T	
	Mean	SD	Mean	SD	Mean	SD
Speed of shot($m*s^{-1}$)						
X	16.13	0.32	15.83	0.3	15.13	0.97
Y	9.96	0.72	12.43	0.83	8.33	0.51
Z	5.4	0.36	7.51	0.28	9.33	0.31
Hitting position (m)						
X	0.18	0.12	0.28	0.11	0.25	0.08
Y	1.08	0.11	1.27	0.2	1.33	0.16
Z	3.13	0.65	3.14	1.02	3.03	0.63
Hitting Angle (°)	16.93	0.17	12.33	0.29	8.13	0.16
The speed of hitting the ball($m*s^{-1}$)	5.36	0.1	5.86	0.26	6.36	0.31
Centroidal distance(m)						
X	0.5	0.1	0.49	0.12	0.49	0.06
Y	0.53	0.12	0.52	0.11	0.55	0.07
Z	0.49	0.11	0.51	0.14	0.5	0.06
Center of gravity(m)						
X	0.34	0.11	0.29	0.13	0.35	0.06
Y	0.3	0.12	0.32	0.1	0.31	0.11
Z	0.25	0.1	0.26	0.11	0.3	0.05
Knee-joint(°)	38.33	1.49	41.63	1.99	39.73	2.14

IV. B. Displacement, velocity characteristics, and analysis of body movements

IV. B. 1) Characteristics and Analysis of Body Center of Gravity Displacement

The player's center of gravity displacement curve is shown in Figure 7. During the player's serving motion, based on the displacement curves and parameters of the center of gravity in the X, Y, and Z directions as reflected in Figure 7, the displacement amplitudes in the Y and Z directions are both relatively small, meaning that the changes in the center of gravity primarily occur in the front-to-back direction. Between 0 and 1.857 seconds—when the body's center of gravity descends from the start of the motion to its lowest point—the displacement amplitude in the X direction is approximately 0.087 meters. The displacement amplitude in the Y direction is approximately 0.014 meters, while the displacement amplitude in the Z direction is approximately 0.028 meters. This indicates that during the period from the player's swing to the lowest point of the squat, the displacement of the body's center of gravity in the Y-direction is relatively small, with the primary changes occurring in the X- and Z-directions, meaning that the body's center of gravity shifts both in the front-to-back and vertical directions. During the subsequent 2.666 seconds, the player transitions from the lowest point of the squat to the moment of ball contact. During this period, the displacement amplitude in the X direction is approximately 0.598 meters. The displacement amplitude in the Y direction is approximately 0.196 meters, while the displacement amplitude in the Z direction is approximately 0.253 meters. It can be observed that during this period, the body's center of gravity begins to stabilize in the Y-direction, meaning that as the player's body rises, it maintains good stability in the lateral direction. As shown in Figure 7, significant changes in the body's center of gravity in the X-direction begin at 1.603 seconds and become more pronounced after 2.648 seconds, particularly after the swing and ball contact, due to the body's follow-through motion.

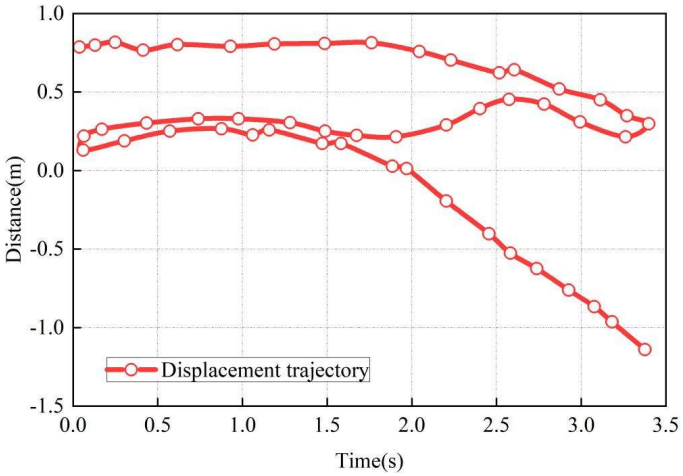

Figure 7: The displacement curve of player's body center of gravity

IV. B. 2) Speed Characteristics and Analysis of Body Center of Gravity

The three-component velocity curves of the player's center of gravity in the X, Y, and Z directions are shown in Figure 8. The characteristics of the three-component linear velocities of the center of gravity in the V_X, V_Y, and V_Z directions during different action phases are listed in Table 4. The selected action phases include: (D1) initial state, (D2) moment when the center of gravity begins to descend, (D3) lowest point of the center of gravity, (D4) the highest point of the racket head during the swing, (D5) the lowest point of the racket head during the swing, (D6) the moment of ball contact, and (D7) the moment the ball is struck. Based on the action characteristics reflected in Figure 8 and Table 4, during the execution of the serve action, the linear velocity characteristics of the player's body center of gravity in the X, Y, and Z directions vary across different action phases.

When the body's center of gravity begins to descend, the corresponding initial velocities are: V_X = 0.086 m/s, V_Y = 0.062 m/s, and V_Z = 0.071 m/s. This indicates that when the player's body begins to descend, the center of mass is not moving strictly along the vertical axis but is also moving in the X and Y directions. When the body descends from the start of the movement to the lowest point, the corresponding velocities of the body's center of gravity are: V_X = 0.441 m/s, V_Y = 0.169 m/s, and V_Z = 0.222 m/s. When the body's center of gravity reaches its lowest point, it is moving at a certain speed in the X, Y, and Z directions, indicating that the body has not come to a complete stop. When the player swings the racket to the highest point of the racket head, the corresponding velocities of the body's center of gravity are: V_X =0.215 m/s, V_Y =0.133 m/s, and V_Z =0.130 m/s. When the racket head reaches its lowest point (“scratching the back” motion), the corresponding velocities of the body's center of gravity are: V_Z =1.068 m/s, V_Y =0.263 m/s, and V_Z =0.72 m/s.

During the player's backswing, the speed of the body's center of gravity in the Z direction reached two peaks, with the final peak occurring precisely at the moment the backswing was completed. At this point, the body's center of gravity also achieved its maximum speed in the X direction during the entire process, indicating that the player had accumulated exceptional explosive power at that moment. At the moment of ball contact, the velocities corresponding to the player's body center of mass when the racket first touches the ball are: V_X = 0.555 m/s, V_Y = 0.452 m/s, and V_Z = 0.111 m/s. When the ball leaves the racket, the corresponding velocities of the player's center of gravity are: V_X =0.481 m/s, V_Y =0.372 m/s, and V_Z =0.027 m/s. From the changes in the data, it can be seen that the velocities in the X and Z directions decrease significantly, especially in the Z direction, indicating a large acceleration in the vertical direction.

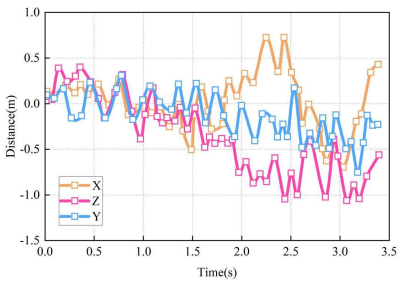

Figure 8: The X, Y, and Z components of the body's center of gravity velocity

Table 4: Three-direction linear velocity characteristics at different action stages

	V_X (m/s)	V_Y (m/s)	V_Z (m/s)
D1	0.000	0.000	0.000
D2	0.101	0.074	0.084
D3	0.452	0.181	0.235
D4	0.235	0.146	0.152
D5	1.089	0.277	0.711
D6	0.573	0.465	0.117
D7	0.492	0.383	0.04

IV. C. Aerodynamic analysis based on a tennis biomechanical model

IV. C. 1) Response of flow field characteristics to tennis ball motion

To analyze the characteristics of the flow field around a tennis ball in different motion states, this paper selects two representative combinations of conditions for analysis: ball speed of 25 m/s and spin speed of 45 rad/s, and ball speed of 25 m/s and spin speed of 65 rad/s. The pressure cloud patterns of the flow field around the tennis ball under each condition are shown in Figure 9.

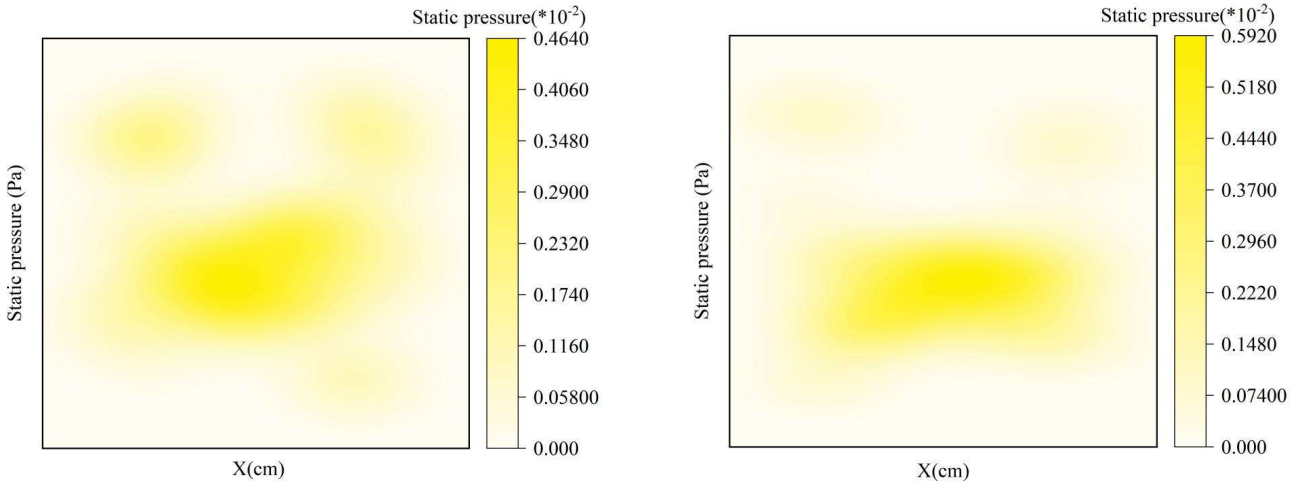

(a) The ball speed is 25m/s and the rotational speed is 45rad/s

(b) The ball speed is 25m/s and the rotational speed is 65rad/s

Figure 9: The pressure of the surrounding flow field under different motion states

The comparison between Figure 9(a) and Figure 9(b) shows that, under the same ball speed, changes in the spin speed of the tennis ball result in significant changes in pressure distribution. As the spin speed increases, the pressure on the lower surface decreases, the pressure difference between the upper and lower surfaces increases, and the location of boundary layer separation shifts toward the leading edge of the tennis ball. The Magnus effect becomes increasingly pronounced as the spin speed of the tennis ball increases. The greater the “downward force” experienced by the ball, the shallower its landing point. When the opponent is positioned forward and preparing to intercept, the player can adopt a spin-heavy strategy to create a rapid descent over the net, thereby increasing the opponent's difficulty in predicting and intercepting the ball.

IV. C. 2) Analysis of aerodynamic parameters of tennis balls

Numerical simulation experiments can provide aerodynamic parameters under different tennis ball rotation speeds and flight speeds, namely the drag coefficient and lift coefficient values. This section focuses solely on the drag coefficient values. Aerodynamic parameters characterize the relationship between the drag and Magnus force acting on the tennis ball and the relative wind speed, aiding in the analysis of the force characteristics and patterns during the ball's flight. The drag coefficient is related to the Reynolds number, while the lift coefficient is related to the rotation rate α. In the simulation experiments under various conditions, the drag coefficient varies with the motion speed and rotation coefficient, as shown in Figure 10. The results of the simulation experiment show that

the drag coefficient increases with the increase of tennis ball speed in a certain Reynolds number range, and when the tennis ball speed is 40m*s-1, the drag coefficient increases to 0.1347. When the rotation speed of the tennis ball increases, the pressure difference between the upper and lower surfaces of the tennis ball changes, and the drag coefficient is basically unchanged (0.03~0.032). The above experimental results show that ball speed has a great influence on the drag coefficient.

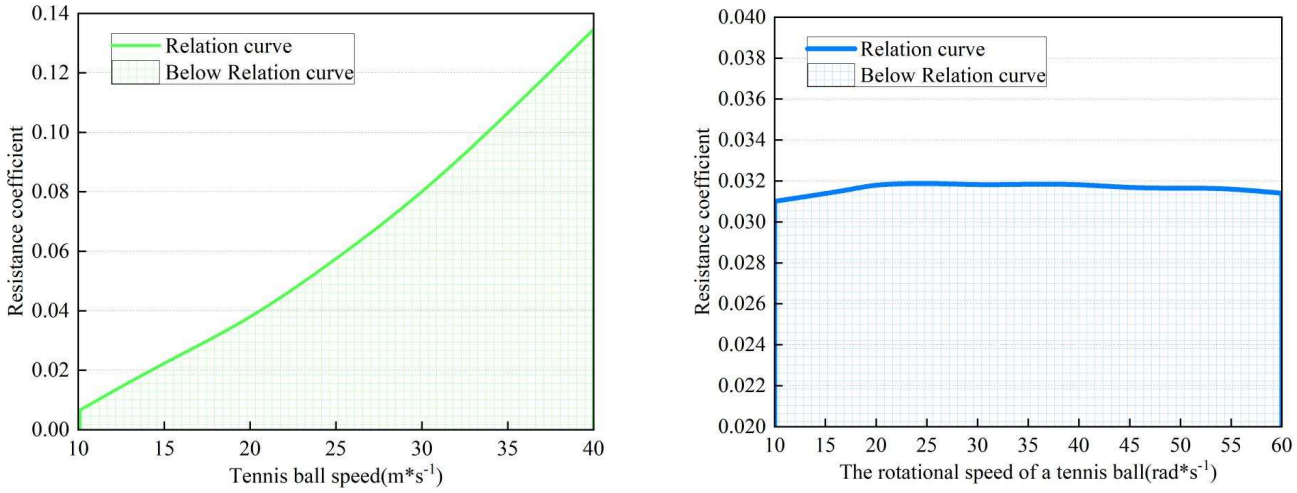

(a) Tennis ball speed and drag coefficient

(b) The rotational speed and resistance coefficient of tennis balls

Figure 10: The relationship between the resistance coefficient and the parameters

V. Conclusion

In terms of the description of the tennis ball serving state, this paper extracts the main forces that affect the trajectory of tennis from the force during tennis movement, describes the tennis movement process by fusing the force situation, designs the mathematical equation of the motion state, and proposes a tennis kinematic model. Taking 10 national first-class tennis players as experimental subjects, based on the displacement characteristics and velocity characteristics of the center of gravity of their bodies during the serving process, the proposed model was used to carry out high-performance parallel calculation. In a certain range of Reynolds number, the drag coefficient increases with the increase of tennis ball speed (when the tennis ball speed reaches 40m*s-1, the drag coefficient increases to 0.1347), while when the tennis ball rotation speed increases, the drag coefficient is basically unchanged (0.03~0.032).

References

[1] Rahim, M. R. A., Shapie, M. N. M., Abdullah, N. M., Parnabas, V., Hasan, H., & Khir, Z. M. (2021). Review on the transformation of tennis development in Malaysia. Malaysian Journal of Sport Science and Recreation (MJSSR), 17(1), 73-88.

[2] Haugen, T. A., Ruud, C., Sandbakk, S. B., Sandbakk, Ø., & Tønnessen, E. (2024). The Training and Development Process for a Multiple-Grand-Slam Finalist in Tennis. International Journal of Sports Physiology and Performance, 19(11), 1247-1255.

[3] Filipcic, A. (2024). Designing a sustainable structure for tennis competitions at national and regional level. ITF Coaching & Sport Science Review, 32(93), 41-45.

[4] Sari, E. G. P., Marheni, E., Damrah, D., & Komaini, A. (2022). Tennis Sports Development at the Bengkulu Tennis School (STB). Kinestetik: Jurnal Ilmiah Pendidikan Jasmani, 6(4), 754-763.

[5] Cahill, G., & MacNamara, Á. (2024). Managing high performance systems in tennis: examining meso and macro factors underpinning player development structures in tennis. International Journal of Sport Management and Marketing, 24(3-4), 313-338.

[6] Thongthanapat, N., & Khamros, W. (2024). Comparing and analyzing elite soft tennis players: Match workload, technique, and action area in high-level competitive games. Journal of Human Sport and Exercise, 19(3), 748-756.

[7] Putri, A. R., & Riyadi, S. (2024). Enhancement of basic tennis technical skills: Game and drill training methods of male athletes reviewed by age group. Journal Sport Area, 9(2), 320-328.

[8] Kramer, T., Huijgen, B. C., Elferink-Gemser, M. T., & Visscher, C. (2017). Prediction of tennis performance in junior elite tennis players. Journal of sports science & medicine, 16(1), 14.

[9] Zhang, C. (2024, June). Machine Learning Algorithm Based Prediction of Players' Scores in Tennis Matches. In 2024 2nd International Conference on Mechatronics, IoT and Industrial Informatics (ICMIII) (pp. 270-273). IEEE.

[10] Chen, H. (2022). A Data Mining - Based Model for Evaluating Tennis Players' Training Movements. Discrete Dynamics in Nature and Society, 2022(1), 8950732.

[11] Fu, M. C., Ellenbecker, T. S., Renstrom, P. A., Windler, G. S., & Dines, D. M. (2018). Epidemiology of injuries in tennis players. Current reviews in musculoskeletal medicine, 11, 1-5.
[12] Rosker, J., & Majcen Rosker, Z. (2021). Skill level in tennis serve return is related to adaptability in visual search behavior. Frontiers in Psychology, 12, 689378.
[13] Zhang, Y., & Chen, Z. (2024). Kinematic differences in forehand serve-receiving techniques of the male tennis players at low and high-speed serves. Scientific Reports, 14(1), 26586.
[14] Martin, C. (2019). Biomechanics of the tennis serve. Tennis medicine: a complete guide to evaluation, treatment, and rehabilitation, 3-16.
[15] Palmer, K., Jones, D., Morgan, C., & Zeppieri Jr, G. (2018). Relationship between range of motion, strength, motor control, power, and the tennis serve in competitive-level tennis players: a pilot study. Sports health, 10(5), 462-467.
[16] Söğüt, M. (2017). A comparison of serve speed and motor coordination between elite and club level tennis players. Journal of Human kinetics, 55, 171.
[17] Robinson, G., & Robinson, I. (2018). Model trajectories for a spinning tennis ball: I. The service stroke. Physica Scripta, 93(12), 123002.
[18] Lambrich, J., & Muehlbauer, T. (2023). Biomechanical analyses of different serve and groundstroke techniques in tennis: A systematic scoping review. PLoS One, 18(8), e0290320.
[19] Meffert, D., O'Shannessy, C., Born, P., Grambow, R., & Vogt, T. (2018). Tennis serve performances at break points: Approaching practice patterns for coaching. European journal of sport science, 18(8), 1151-1157.
[20] Brocherie, F., & Dinu, D. (2022). Biomechanical estimation of tennis serve using inertial sensors: A case study. Frontiers in Sports and Active Living, 4, 962941.
[21] Li, X., & Huang, P. (2020). Simulation of tennis serve behavior based on video image processing and wireless sensor technology. EURASIP Journal on Wireless Communications and Networking, 2020(1), 137.
[22] Hu, R. (2023). IoT-based analysis of tennis player's serving behavior using image processing. Soft Computing, 27(19), 14413-14429.
[23] Carboch, J., Tufano, J. J., & Süss, V. (2018). Ball toss kinematics of different service types in professional tennis players. International Journal of Performance Analysis in Sport, 18(6), 881-891.
[24] Yu, S. (2022). Tennis Serve Trajectory Capture Algorithm Based on Wavelet Multiscale Decomposition. Mathematical Problems in Engineering, 2022(1), 8290282.